Mathematical Biosciences and Engineering

https://www.aimspress.com/journal/mbe

MBE, 21(11): 7501–7529.
DOI: 10.3934/mbe.2024330
Received: 12 July 2024
Revised: 17 October 2024
Accepted: 29 October 2024
Published: 11 November 2024

Research article

Mathematical modeling of the parasitism and hyperparasitism increase on *Halyomorpha halys* eggs in a five-year survey in Northern Italy

Ezio Venturino[1,2,*], Francesco Cantaloni[1], Luciana Tavella[3], Silvia Moraglio[3] and Francesco Tortorici[3]

[1] Dipartimento di Matematica "Giuseppe Peano", Università degli Studi di di Torino, via Carlo Alberto 10, 10123 Torino, Italy; member of the research group GNCS.

[2] Laboratoire Chrono-Environnement, Université de Franche-Comté, 16 route de Gray, Besançon, 25030, France

[3] Dipartimento di Scienze Agrarie, Forestali e Alimentari, Università degli Studi di Torino, largo Paolo Braccini 2, 10095 Grugliasco (TO), Italy

* **Correspondence:** Email: ezio.venturino@unito.it.

Abstract: The invasive stink bug *Halyomorpha halys* has become an important pest of many crops, causing severe economic losses to farmers. Control of the pest mainly relies on multiple applications of broad-spectrum insecticides, undermining the integrated pest management programs and causing secondary pest outbreaks. In the native area, egg parasitoids are the main natural enemies of *H. halys*, among which *Trissolcus japonicus* is considered the predominant species. In Italy, adventive populations of *T. japonicus* and *Trissolcus mitsukurii*, another egg parasitoid of *H. halys* in Japan, have established themselves. These two species, together with the indigenous *Anastatus bifasciatus*, are capable of attacking the eggs of the exotic host. Focusing on the situation in Northern Italy, where also the hyperparasitoid *Acroclisoides sinicus* is present, a discrete-time model is developed for the simulation of the pest evolution. It is based on actual field data collected over a timespan of five years. The simulations indicate that egg parasitoid by themselves do not suppress populations to non-pest levels, but can play an important role in reducing their impact. Both the data from the five-year surveys and those available in the literature are used in the model. It has some limitations in the fact that climatic conditions were not considered, while more accurate simulations could be performed with additional collection of field data, which at the moment are based on partial field observations not sampled at the same sites.

Keywords: invasive species; discrete dynamical model; agricultural pest control; in-silico simulations; equilibria feasibility and stability

1. Introduction

Halyomorpha halys (Stål) (Hemiptera: Pentatomidae) is an invasive stink bug introduced from Asia into North America, Europe, and Chile [1–3]. In Italy, invasion may have occurred from two different pathways, both from Switzerland and from Asia and/or North America [4]. In the invaded areas, *H. halys* has become an important pest of many crops, causing severe economic losses due to its feeding activity mainly on developing fruits and seeds, such as apples, pears, peaches, nectarines, tomatoes, peppers, sweet corn, soybean and hazelnuts [1, 5]. In particular, in Italy, under the current climatic conditions, the species is able to complete two generations per year and has shown very high reproductive rates for both generations, with massive outbreaks starting from the summer, confirming that it is a threat for agricultural production in southern Europe [6]. Control of the pest mainly relies on multiple applications of broad-spectrum insecticides, nullifying the integrated pest management programs largely adopted in Italy, and causing secondary pest outbreaks [5]. For this reason, as a long-term solution, classical biological control based on the use of parasitoids has been considered in the United States and Europe [1]. Parasitoids are insects with a parasitic larval stage (juveniles) that develops by feeding on another insect called the host, and in our case feeding on a single egg of *H. halys*. Unlike parasites, at the end of their development, parasitoid larvae kill their host like a predator, but they only need one host to complete their development. Then, the resulting adult is a free-living insect. Therefore, a parasitoid adult, and not a stink bug nymph, will emerge from an egg attacked by *Anastatus bifasciatus* (Geoffroy) (Hymenoptera: Eupelmidae) or by *Trissolcus japonicus* (Ashmead) (Hymenoptera: Scelionidae) [7]. Indeed, in Europe, an indigenous egg parasitoid, *A. bifasciatus*, is able to attack *H. halys* eggs, but without achieving effective containment of pest populations [8, 9]. In the native area, egg parasitoids are the primary natural enemies of *H. halys*, and *T. japonicus* is considered the predominant species among the egg parasitoid complex of *H. halys* in China and Japan [10, 11]. Therefore, *T. japonicus* has been selected as a candidate for classical biological control both in North America and Europe [12–14].

Currently, field releases of *T. japonicus* have been authorized in Italy starting from 2020. However, before any field release, adventive populations of *T. japonicus* were detected in North Italy from 2018, as well as adventive populations of *Trissolcus mitsukurii* (Ashmead) (Hymenoptera: Scelionidae) [9, 15]. This latter species, known as an egg parasitoid of *H. halys* in Japan [11], has been found in Northern Italy since 2016 [16], and has also been considered as a promising candidate for biological control [17]. Both *T. japonicus* and *T. mitsukurii* have successfully established in Northern Italy, even before the release of *T. japonicus* was authorized as a part of the national classical biological control program, and contribute to the *H. halys* control together with the native *A. bifasciatus* [18]. The indigenous and exotic parasitoids can act synergistically in the biological control of *H. halys* and, in case of competition, *T. japonicus* and *A. bifasciatus* have been shown to be counterbalanced, the former being a superior extrinsic competitor (by guarding eggs), the latter being a superior intrinsic competitor, successfully emerging from eggs that were previously parasitized by *T. japonicus* [19]. Finally, a hyperparasitoid, *Acroclisoides sinicus* (Huang and Liao) (Hymenoptera: Pteromalidae), which develops in *H. halys* eggs previously parasitized by the *Trissolcus* species, is also present in Northern Italy [20, 21]. Hyperparasitoids, or secondary parasitoids, act as parasitoids, but develop on primary parasitoids: an *A. sinicus* female lays eggs in the *H. halys* eggs that have already been attacked to develop on the larvae of *Trissolcus* spp. The offspring of the hyperparasitoid

causes the death of the primary parasitoid. An *A. sinicus* adult will emerge from the attacked *H. halys* eggs, [22]. The interaction between parasitoids and hyperparasitoids can play a key role in determining the overall effectiveness of biological control of *H. halys*. As little information has yet been available on the *Trissolcus* spp. impact on *H. halys* populations, and on the *A. sinicus* impact on *Trissolcus* spp. populations, field surveys were carried out in Piedmont, North-western Italy, from 2017 to 2021 to assess the impact of parasitoids and hyperparasitoids. Both the data from the five-year surveys and those available in the literature are used in the model proposed here.

The paper is organized as follows. Section 2 contains all the various steps in the model construction, starting from the description of the field data gathering. It is followed by the overview of the simulations organization. Their results are presented and thoroughly discussed in Section 4. Section 5 reports the main findings on the equilibria of the model. Some remarks on the results obtained and the model limitations conclude the paper. The mathematical details of the feasibility and stability of the equilibria of the general model are presented in the Appendix A, while its Subsection A.3 analyzes a special simplified situation.

2. Model formulation

2.1. Data collection

Seasonal abundance of *H. halys* adults was monitored weekly from May to October, at 40 sites with pheromone-baited traps (Dead-Inn Pyramid Trap - 4 ft. height, AgBio Inc., baited with Pherocon BMSB Dual Lure, Trécé Inc.), from 2018 to 2021. The traps were placed in the same locations, distributed throughout Piedmont, NW Italy, and captures were checked weekly from May to October. The collection points are reported in Figure 1, where the red dots represent the eggs collection points and the blue ones the location of the traps. Seasonal abundance of the parasitoids *Trissolcus* spp., *A. bifasciatus*, and the hyperparasitoid *A. sinicus* was monitored monthly from June to August from 2017 to 2021 by collecting field-laid *H. halys* eggs with one-hour visual inspection, at 6 sites in 2017, at an additional 3 sites (9 in total) in 2018 and at an additional 6 sites (15 in total) in 2019, 2020 and 2021. All eggs were reared in laboratory, and the number of i) *H. halys* nymphs, ii) *A. bifasciatus* adults, iii) *Trissolcus* spp. adults, and iv) *A. sinicus* adults which emerged from eggs were counted, discarding unhatched or preyed eggs.

2.2. Basic interactions

The mutual interactions of *H. halys* and its parasitoids, described in the Introduction are summarized in Figure 2. We use I to denote the hyperparasitoid *A. sinicus*, A to indicate the indigenous parasitoid *A. bifasciatus*, T to denote the combined populations of the parasitoids *T. japonicus* and *T. mitsukurii*, while C indicates the invasive pest *H. halys*. In addition, because parasitization occurs on *H. halys* eggs, these must be accounted in the formulation. Because the life cycle of these insects can be expressed in weeks, as illustrated in Tables 2 and 3, we chose the week as the time unit. A further consequence is that a discrete dynamical system formulation naturally arises, instead of a possible continuous one.

The various population dynamics are essentially represented by three terms, denoting reproduction R^X, intraspecific competition b_X, and natural mortality m_X, where $X \in \{I, A, T, C\}$ indicates the specific population under consideration. Natural mortality represents the mortality rate within a population,

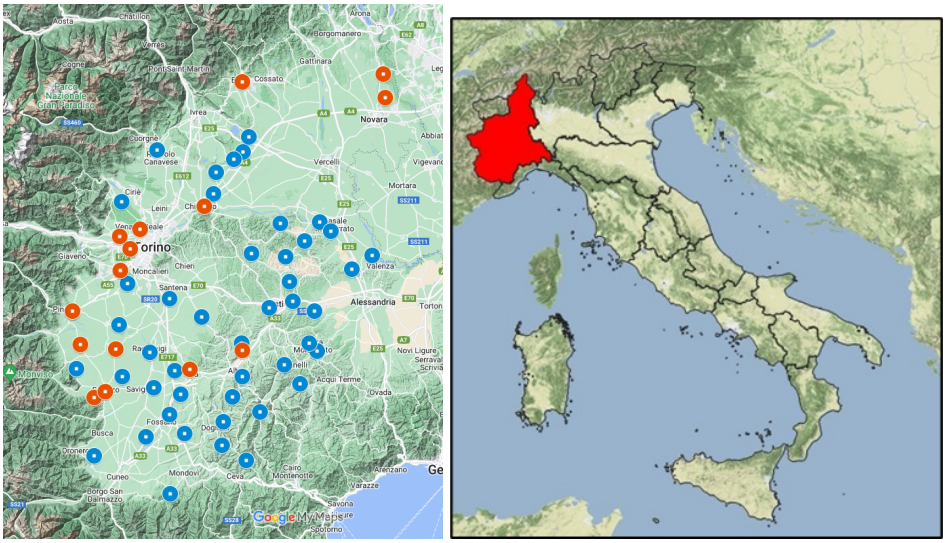

Figure 1. Left frame: sites of field data collection in Piedmont (NW Italy): the red dots represent the sites of field eggs collection and the blue ones sites with traps. Right frame: Piedmont in Italy.

in this case of adult insects, that occurs in the absence of external factors such as natural enemies, diseases, or human intervention. It is obtained as the reciprocal of the average lifetime of a healthy insect, respectively. The *H. halys* reproduction function will be derived from field-collected egg data, and therefore must be time-dependent. The reproduction function for the other insects are based on *H. halys* egg counts, so that they are also time-dependent. As mentioned above, recall that the mortalities are easily obtained as the reciprocal of the average lifetimes of each species, which are known from the literature, [27, 28] for A, [23, 30] for the two T species and [24] for C. For each population $X \in \{I, A, T, C\}$ let X_n denote its value at time $t = n$ and let $\Delta X_n = X_{n+1} - X_n$ be the increment over the time interval $[n, n + 1]$. The discrete model can thus be written as

$$\begin{aligned} \Delta I_n &= R_n^I - b_I I_n^2 - m_I I_n, \\ \Delta A_n &= R_n^A - b_A A_n^2 - m_A A_n, \\ \Delta T_n &= R_n^T - b_T T_n^2 - m_T T_n, \\ \Delta C_n &= R_n^C - b_C C_n^2 - m_C C_n. \end{aligned} \tag{2.1}$$

The model represents the parasitoid-host interactions shown in Figure 2. However, note that no terms for these interactions appear in the equations formulation. This is due to the fact that the damage that some insects cause to the other ones occurs only via the parasitization of their eggs. Therefore, it is very important that this mechanism be correctly depicted in the model, as we show in the next section.

2.3. Egg parasitization

The main effort in the model construction lies in the mathematical description of the egg parasitization. Let s_C denote the sex ratio of *A. sinicus*. Eggs laid by a female *H. halys* are $C_f = s_C C$. However, not all of them are "healthy"; E represents the per capita fraction of healthy eggs that are

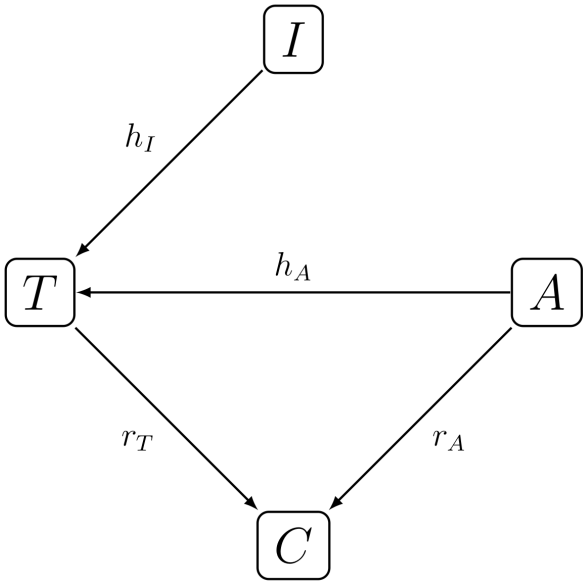

Figure 2. Basic scheme of the model. The full meanings of the parameters are contained in Table 1: basically, h_I and h_A are the egg mass fraction already parasitized by T from which, respectively, I emerges or A emerges, while r_A and r_T are the parasitization rates of A and T. Recall also that hyperparasitoid I affects only *Trissolcus T* because it develops in *H. halys* eggs previously parasitized by *Trissolcus* species, [20, 21]. Also, as stated in the body of the paper, the indigenous and exotic parasitoids act synergistically in the biological control of *H. halys* and, in case of competition, *T. japonicus* and *A. bifasciatus* have been shown to be counterbalanced, the former being a superior extrinsic competitor (by guarding eggs) and the latter being a superior intrinsic competitor, successfully emerging from eggs that were previously parasitized by *T. japonicus* [19].

available for parasitization, so that their total number is EC_f. To obtain those that hatch and give new *H. halys* individuals, from these we need to subtract those parasitized by *Trissolcus* spp. and *A. bifasciatus*, indicated by the terms r_T and r_A in the equation below. We thus obtain

$$R^C = s_C EC[1 - r_T - r_A]. \tag{2.2}$$

Further, since only females lay eggs, it is important to consider the sex ratio. The parameter s_T denoting the sex ratio (females over the whole population) for *Trissolcus* spp. is known, $s_T = 0.87$ [23]. For *H. halys* in general the sex ratio is assumed as $s_C = 0.5$ [24].

We now discuss the parasitization process.

Considering for the moment that parasitization is due to *Trissolcus* spp., the total number of parasitized eggs would be obtained by multiplying the per capita parasitization $\widetilde{r}_T$ of T with the total female population of *Trissolcus* spp. $T_f = s_T T$, where s_T denotes the sex ratio of *Trissolcus*, namely $R_T = EC_f \widetilde{r}_T T_f$. In this way, however, if the parasitization rate were higher than one, i.e, $\widetilde{r}_T T > 1$, the total number of emerging *Trissolcus* adults would exceed the total number of eggs laid by *H. halys*, which of course cannot be. Therefore, we need to correct this approach.

For this purpose, we need to consider the parasitization rate as a function of the parasitizing agent population. In the discussion above, this corresponds to taking $\widetilde{r}_T = r_T(T)$. The function $r_T(T)$ should

have a specific form, namely it should be bounded from above. Such choice is represented by a Holling type II-like function, i.e.,

$$r_T(T) = \beta_T \frac{s_T T}{q_T + s_T T}, \tag{2.3}$$

where q_T^{-1} represents the slope at the origin of the parasitization rate. In this way, $0 \leq r_T < 1$. Here, $0 \leq \beta_T \leq 1$ represents the reproduction effectiveness. The two extreme values denote particular situations. For the case in which *Trissolcus* spp. are present, but no eggs parasitized by them are found in the field samples, we set $\beta_T = 0$. Note that if *H. halys* eggs were scarce, the presence of *Trissolcus* spp. could be inferred by sampling the adults with traps, beating sheets, or other methods. If instead all females of *Trissolcus* spp. parasitize all the available eggs, we set $\beta_T = 1$.

Anastatus bifasciatus behaves in a similar way on *H. halys* eggs. We can thus introduce corresponding functions and notations. However, like *A. sinicus*, it can also parasitize *Trissolcus* spp. This hyperparasitization must be described in the same way, considering hyperparasitization as the product of two different parasitization processes. Specifically, for *A. bifasciatus* it is necessary to distinguish between the parasitization rate $r_A(A)$ on *H. halys* and the one on *Trissolcus* spp., denoted by $h_A(A)$. In view of the previous remarks, we can thus write

$$r_A(A) = \frac{\beta_A s_A A}{q_{A,C} + s_A A}, \quad h_A(A) = \frac{\beta_A s_A A}{q_{A,T} + s_A A}, \quad h_I(I) = \frac{\beta_I s_I I}{q_I + s_I I}, \tag{2.4}$$

with $q_T, q_{A,C}, q_{A,T}, q_I > 0$. Their reciprocals are the slopes at the origin of the parasitization or hyperparasitization rates. Note that different notations have been used for the parameters in the denominator: $q_{A,C}$ and $q_{A,T}$ stand for the parasitization and hyperparasitization due to *A. bifasciatus*, respectively. In addition to the ones mentioned above, the sex ratios also of these insects are known [21, 25].

In summary, we have

$$s_C = 0.5, \quad s_T = 0.87, \quad s_A = 0.49, \quad s_I = 0.73. \tag{2.5}$$

Further, from (2.1) the reproduction rates $r_X(X)$, $X \in \{T, A\}$ and $h_X(X)$, $X \in \{A, I\}$ must be nonnegative, so that the following inequalities must be satisfied,

$$1 - h_A(A) - h_I(I) \geq 0, \quad 1 - r_A(A) - r_T(T) \geq 0, \tag{2.6}$$

which become

$$h_A(A) + h_I(I) \leq 1, \quad r_A(A) + r_T(T) \leq 1. \tag{2.7}$$

Let us denote by E_X, $X \in \{I, A, T, C\}$ the newly emerged offsprings of species X from a single egg mass. Let also p_X denote the respective rates. They are given by

$$p_I := \frac{E_I}{E}, \qquad p_A := \frac{E_A}{E}, \qquad p_T := \frac{E_T}{E}, \qquad p_C := \frac{E_C}{E}, \tag{2.8}$$

so that

$$p_I + p_A + p_T + p_C = 1 \tag{2.9}$$

Since the rates p_X are known from available field data, we need to find further conditions on the rates $r_X(X)$, $X \in \{T, A\}$ and $h_X(X)$, $X \in \{A, I\}$ so that they are feasible. To simplify the notation, for the rest of this section we drop the explicit dependence of these functions on the respective population sizes.

Now $R_T h_I$ is the per capita hyperparasitization rate p_I. Instead, $r_A + r_T h_A$ is the sum of the direct per capita parasitization rate of A on C, to which we add the hyperparasitization rate of A on T, to get p_A. Similarly, $r_T(1 - h_A - h_I)$ represents the per capita net parasitization rate of T on C, where we have discounted the hyperparasitizations of A and I. It therefore represents p_T. Also, $1 - r_A - r_T$ represents the per capita net reproduction rate of C, adjusted for the parasitizations of A and T, and thus gives p_C. These considerations lead to the following relationships

$$r_A = 1 - r_T - p_C, \quad h_A = 1 - \frac{p_I + p_T}{r_T}, \quad h_I = \frac{p_I}{r_T}. \tag{2.10}$$

Since the rates must lie in the interval [0, 1], the following constraints must be satisfied:

$$r_T \geq p_I, \quad r_T \geq p_I + p_T, \quad r_T \leq 1 - p_C, \tag{2.11}$$

where the second one is more restrictive than the first one. Ultimately, r_T must lie in the following interval

$$r_T \in [p_I + p_T,\ 1 - p_C] = \frac{1}{E}[E_I + E_T,\ E - E_C]. \tag{2.12}$$

Note that this interval is nonempty; from (2.9) we have indeed $p_I + p_A + p_T = 1 - p_C$ and since $p_A \in [0, 1]$ we have $p_I + p_T \leq 1 - p_C$, the required result. In summary, the required feasibility conditions for the rates are

$$h_I \in [0, 1 - h_A], \quad r_T \in [p_I + p_T, 1 - \max\{p_C, r_A\}]. \tag{2.13}$$

Now *A. sinicus* reproduces because it parasitizes the eggs of *H. halys* already parasitized by *Trissolcus* spp., [19], so that we can state

$$R^I = s_C E C r_T h_I. \tag{2.14}$$

Instead, *A. bifasciatus* can parasitize the eggs of *H. halys* at rate $s_C E C r_A$ and also those parasitized by *Trissolcus* spp. at rate $s_C E C r_T h_A$, overall giving

$$R^A = s_C E C [r_A + r_T h_A]. \tag{2.15}$$

Finally, *Trissolcus* spp. attack the eggs of *H. halys*

$$R^T = s_C E C r_T [1 - h_A - h_I]. \tag{2.16}$$

However, a further consideration should be made. Indeed, we have considered the reproduction process whereby insects emerge from the available *H. halys* eggs. It should be noted that from egg to adulthood, insects go through developmental stages that are different when heterometabolous, such as *H. halys*, and holometabolous, such as parasitoids and hyperparasitoid. This whole process is not at all considered in the modeling procedure: juvenile stages do not appear explicitly in the model.

However, these stages are still affected by natural mortality, which reduces the eggs produced by factors σ_Y, $Y \in \{I, A, T, C\}$. These must therefore be included in the equation formulation.

Putting together the above considerations and (2.2), (2.14)–(2.16), the system to be studied is therefore

$$\begin{aligned} I_{n+1} &= I_n + \sigma_I s_C E C_n r_T(T_n) h_I(I_n) - b_I I_n^2 - m_I I_n, \\ A_{n+1} &= A_n + \sigma_A s_C E C_n [r_A(A_n) + r_T(T_n) h_A(A_n)] - b_A A_n^2 - m_A A_n, \\ T_{n+1} &= T_n + \sigma_T s_C E C_n r_T(T_n)[1 - h_A(A_n) - h_I(I_n)] - b_T T_n^2 - m_T T_n, \\ C_{n+1} &= C_n + \sigma_C s_C E C_n [1 - r_A(A_n) - r_T(T_n)] - b_C C_n^2 - m_C C_n. \end{aligned} \tag{2.17}$$

The parameters of the system (2.17) are listed in Table 1 together with their meanings.

3. Simulation settings

The simulations were performed using our data collected in the field over the past five years.

A few caveats are necessary to describe the procedure used to overcome some shortcomings that might arise in the simulations.

Table 1. Model parameters and their interpretation.

$\gamma \in [0, 1]$	fraction of eggs from which no adult insects emerge
$0 \leq \tilde{E}$	average of all eggs collected in a week in egg mass
$0 \leq E = (1 - \gamma)\tilde{E}$	healthy eggs in egg mass, from which *H. halys* or its parasitoids emerge
s_I	sex ratio of *A. sinicus*, [21]
s_A	sex ratio of *A. bifasciatus*, [25]
s_T	sex ratio of *Trissolcus*, [23]
s_C	sex ratio of *H. halys*, [24]
$h_I := h_I(I) \in [0, 1]$	egg mass fraction already parasitized by T, from which I emerges
$h_A := h_A(A) \in [0, 1]$	egg mass fraction already parasitized by T, from which A emerges
$r_A := r_A(A) \in [0, 1]$	parasitization rate of A, i.e. egg mass fraction from which A emerges by parasitizing C
$r_T := r_T(T) \in [0, 1]$	parasitization rate of T, i.e. egg mass fraction parasitized by T, i.e. sum of newly emerged T and its hyperparasitoids
$0 \leq b_*$	intraspecific competition rate of species $*$
$m_* \in [0, 1]$	mortality rate of species $*$
$\beta_* \in [0, 1]$	(hyper-)parasitization rate of species $*$
$0 < q_*^{-1}$	slope at the origin of (hyper-)parasitization rate

Because the information on the egg masses did not cover the entire timespan, but had some gaps, a spline cubic interpolation on the two closest available data points was performed to obtain the values

at times when they were missing. Furthermore, at the beginning and end of the season, the number of laid eggs was set to zero, through an interpolation procedure.

The beginning of the season, when *H. halys* females start oviposition, is assumed to be the 19-th week of the year, i.e., the second or third week of May [6]. The end before the onset of winter diapause is set at the 42-nd week, i.e., the third week of October [6]. Trap catch data before the 19-th week were discarded, as most individuals are still in diapause or have not yet started laying eggs.

Furthermore, most insect data other than those collected in the field, i.e., field collected eggs and trap catch counts, come from laboratory experiments, and therefore may differ from those occurring in the field [23,24,27–30] as specified below in detail in Subsection 3.1. Another limitation is that population data are just estimates on the actual numbers of *H. halys* in the environment, being calculated as an average of insects captured at various sites, which differ greatly in location and environmental conditions. A similar observation applies to parasitoids, which count an average number of those that emerge from field collected eggs. This entails that the differences between data and simulation values may sometimes be large.

The simulations ran starting from the year 2017, and iterated. In particular, note that all the populations with which the following year begins come from the corresponding values obtained at the end of the current year, in the fall, for which a fixed fraction is deducted that should account for their mortality during overwintering [6, 26]. This is an important point, since each year the climatic conditions may change, and taking a constant value for winter mortality does not adequately mimic what happens in reality. However, little information is available and therefore this assumption attempts to surrogate the missing estimate. A similar observation can be made on intraspecific competition rates, which cannot be measured in the field.

3.1. Developmental period and average female longevity

The data of Table 2 come from [27] for I, [28] for A, [23, 29, 30] for the two T species and [24] for C.

Table 2. Biological traits of the insects under study.

Insect	Time from eggs to adulthood	Mean longevity
Hyperparasitoid I	2 weeks	7 weeks
Indigenous parasitoid A	2 weeks	14 weeks
Exotic parasitoids T	2 weeks	6 weeks
H. halys C	4 weeks	1 year

Note that in Table 2 the hyperparasitoid I lays eggs within those of C that are already parasitized one week earlier by T. It takes thus 3 more weeks to emerge. Further, the oviposition period of A is about 46 days, followed by a further life period of 17.8 days in which oviposition does not occur [28]. Thus, in the simulations the average lifetime is approximated to 14 weeks, see Table 2. We assume that hyperparasitization of A on C occurs within the first 3 days after oviposition.

Table 3 reports the temporal sequence of the various events within a single generation. Data of this table come from [27] for I, from [28] for A, from [23] for the two T species and from [24] for C. Finally, note that in Table 3 new individuals are accounted for only when they become adult and thereby are able to reproduce.

Table 3. Temporal sequence of the life cycle events of the insects under study.

species	initial week 0	week 1	week 2	week 3	week 4
C	Oviposition	Nymph emergence			Adult emergence
T	Oviposition in *C* eggs		Adult emergence		
A	Oviposition in *C* eggs		Adult emergence		
I		Oviposition in *C* eggs parasitized by *T*		Adult emergence	

3.2. Egg mass data

Tables 4–8 contain the mean number of eggs per egg mass from which *H. halys* or one of its parasitoids emerged, considering all the egg masses collected in each week at sites in which at least two egg masses were present, from 2017 to 2021. Data of Table 4 come from field surveys in 2017, as it is the case for the following tables and the following years. Recall also that E represents healthy eggs, i.e., neither broken, nor preyed, nor parasitized by other species, while E_X, $X \in \{I, A, T, C\}$ represents the average number of each respective species emerged from a single egg mass.

Table 4. Year 2017. E represents healthy eggs, i.e., neither broken, nor preyed, nor parasitized by other species, while E_X, $X \in \{I, A, T, C\}$ represents the average number of each respective species emerged from a single egg mass.

week	$\mathbf{E}$	$\mathbf{E_I}$	$\mathbf{E_A}$	$\mathbf{E_T}$	$\mathbf{E_C}$
24-th	25.3	0	23	0	2.3
25-th	21.5	0	12.8	0	8.7
27-th	18	0	7.5	0	10.5
29-th	22.2	0	8.2	0	14
30-th	20.3	0	5.1	0	15.2
31-st	24.2	0	4	0	20.2
34-th	18.8	0	16.8	0	2
35-th	13.9	0	11.3	0	2.6
37-th	11	0	5.5	0	5.5

Table 5. Year 2018. E represents healthy eggs, i.e., neither broken, nor preyed, nor parasitized by other species, while E_X, $X \in \{I, A, T, C\}$ represents the average number of each respective species emerged from a single egg mass.

week	**E**	$\mathbf{E_I}$	$\mathbf{E_A}$	$\mathbf{E_T}$	$\mathbf{E_C}$
22-nd	20	0	0	0	20
24-th	6.5	0	0	0	6.5
26-th	11.5	0	0	0	11.5
27-th	19.4	0	0	0	19.4
28-th	19	0	0	0	19
29-th	16.1	0	0.2	0	15.9
30-th	15.4	0	0	0	15.4
31-st	21.9	0	0	0	21.9
34-th	17.9	0	0.1	0.4	17.4
35-th	7	0	0	0	7
37-th	18.9	0	0.7	0.8	17.4
38-th	20.9	0	0	0	20.9

Table 6. Year 2019. E represents healthy eggs, i.e., neither broken, nor preyed, nor parasitized by other species, while E_X, $X \in \{I, A, T, C\}$ represents the average number of each respective species emerged from a single egg mass.

week	**E**	$\mathbf{E_I}$	$\mathbf{E_A}$	$\mathbf{E_T}$	$\mathbf{E_C}$
24-th	22.1	0	0	1.3	20.8
25-th	21.7	0	4.2	1.4	16.1
26-th	22.2	0	4.5	2.5	15.2
27-th	25	0	0	0	25
28-th	24	0	0	0	24
30-th	20.2	0	8.3	1.7	10.2
32-nd	16.3	0	9	7.3	0
33-rd	18.9	0	4.3	12.6	2
34-th	20.4	0	5.1	5	10.3
35-th	18.7	0	13.7	2.2	2.8

Table 7. Year 2020. E represents healthy eggs, i.e., neither broken, nor preyed, nor parasitized by other species, while E_X, $X \in \{I, A, T, C\}$ represents the average number of each respective species emerged from a single egg mass.

week	**E**	$\mathbf{E_I}$	$\mathbf{E_A}$	$\mathbf{E_T}$	$\mathbf{E_C}$
23-rd	20.7	0	0	8.7	12
24-th	26	0	0	16.7	9.3
25-th	24	0	0	0	24
26-th	23	0	3.2	6	13.8
27-th	16.4	0	4	3.8	8.6
28-th	18.1	0	6.3	4.8	7
29-th	18.5	0	4.5	3.3	10.7
30-th	18.3	0	8.3	0.3	9.7
31-st	23.4	0	1.6	2	19.8
32-nd	22	0	2.7	4.4	14.9
33-rd	21.6	0	2.5	3.7	15.4
34-th	19.3	0	3.7	10.3	5.3
35-th	19.3	0.2	4.9	4.9	9.3
36-th	16.5	0	5.8	9.7	1
37-th	18	0	14.5	0	3.5

Table 8. Year 2021. E represents healthy eggs, i.e. neither broken, nor preyed, nor parasitized by other species, while E_X, $X \in \{I, A, T, C\}$ represents the average number of each respective species emerged from a single egg mass.

week	**E**	$\mathbf{E_I}$	$\mathbf{E_A}$	$\mathbf{E_T}$	$\mathbf{E_C}$
24-th	21.5	0	1.2	3.3	17
25-th	19.1	0	2.3	14.4	2.4
26-th	19.2	0.1	0.2	4.2	14.7
28-th	22.7	0	1.6	0	21.1
30-th	20	0	4.3	5.2	10.5
31-st	16.2	0	3	0	13.2
32-nd	22.8	0.1	1.9	10.4	10.4
33-rd	19.1	0.4	3.2	9.2	6.3
34-th	20.2	2.4	5.6	9.7	2.5
35-th	15.2	4	0.9	8.5	1.8
36-th	13.5	1.5	2.5	9.5	0

3.3. Trap data

Tables 9–12 contain the mean numbers of *H. halys* adults found per trap and per week at all sites from 2018 to 2021.

Table 9. Year 2018.

week no.	19-th	20-th	21-st	22-nd	23-rd	24-th	25-th	26-th
Trap count	27.5	29.3	25.8	33.6	14	28.4	21.1	14.1
week no.	27-th	28-th	29-th	30-th	31-st	32-nd	33-rd	34-th
Trap count	11.2	7	8.9	15	37.4	42.2	36.3	45
week no.	35-th	36-th	37-th	38-th	39-th	40-th	41-st	42-nd
Trap count	32.9	29.8	39.7	61.1	93.3	109.7	102.9	86.8

Table 10. Year 2019.

week no.	21-st	22-nd	23-rd	24-th	25-th	26-th	27-th	28-th
Trap count	48.9	48.1	73.2	41	45.3	51.1	31	18.5
week no.	29-th	30-th	31-st	32-nd	33-rd	34-th	35-th	36-th
Trap count	14.4	23.2	24.2	45.8	46.6	38.1	44.5	37.5
week no.	37-th	38-th	39-th	40-th	41-st	42-nd		
Trap count	35.6	51.8	67.5	96.5	79.1	72.7		

Table 11. Year 2020.

week no.	21-st	22-nd	23-rd	24-th	25-th	26-th	27-th	28-th
Trap count	24.3	23.1	22.6	17.3	10.4	13.4	11.7	6.3
week no.	29-th	30-th	31-st	32-nd	33-rd	34-th	35-th	36-th
Trap count	5.1	5.2	4.5	9.6	9.6	14.3	15.8	16.3
week no.	37-th	38-th	39-th	40-th	41-st	42-nd		
Trap count	22.9	37.9	60.1	42.4	61.1	71.5		

Table 12. Year 2021.

week no.	19-th	20-th	21-st	22-nd	23-rd	24-th	25-th	26-th
Trap count	12.4	7	16.7	23.4	20.6	20.5	17.3	13.1
week no.	27-th	28-th	29-th	30-th	31-st	32-nd	33-rd	34-th
Trap count	16.1	8.5	7.9	10.2	16.3	27.1	27.4	25.5
week no.	35-th	36-th	37-th	38-th	39-th	40-th	41-st	42-nd
Trap count	23	26.7	29.1	46.3	50.7	57.5	47.5	31.8

4. Simulation results

Because the initial value of the *H. halys* population at the beginning of the year 2017 is not available, we assumed it to be of the same order of the one assessed by traps in the following years, of the order of 100. Since no T is found in the egg masses, but only A is present, and only a fraction of them parasitizes C, the initial condition for the latter in the year 2017 is set to a smaller hypothetical value than the one for *H. halys*. We thus take

$$I_0 = 0, \quad A_0 = 10, \quad T_0 = 0, \quad C_0 = 100. \tag{4.1}$$

In these simulations, the intraspecific competition rate b_C is not known. For the years 2018–2021, it is estimated by a regression procedure based on the minimization of the discrepancy between the simulations results and the actual field data. For the year 2017 instead, the value has been assessed as the one that minimizes the difference between the final value at the end of the fall, discounted for the winter mortality, and the initial population in the following spring. Overwintering survival data in the literature are very variable depending on the temperature and many other factors, 14, 23 and 61%, respectively in [6, 31, 32]. We therefore assumed a mean data of 33% of overwintering survival. The whole argument is repeated in the following years. Based on each insect average lifetime (Table 2), the various mortalities are set to

$$m_I = \frac{1}{7}, \quad m_A = \frac{1}{14}, \quad m_T = \frac{1}{6}, \quad m_C = \frac{1}{52}. \tag{4.2}$$

The value b_C is calculated for *H. halys* as the value that minimizes, in the sense of least squares, the discrepancy of the simulations results with the actual trap data for this species. Because no information on the intraspecific competition of the other populations is available, the values of the coefficients b_I, b_A and b_T are set to the same value b_C.

As discussed at the end of Subsection (2.3), we need to account for the natural mortality of the juvenile stages. We assume a weekly loss of 50%, which leads from the initial number of laid eggs to a lower number of adults. This implies for *H. halys* a reduction factor $\sigma_C = 0.07$ over the whole four week-period to reach the adult stage, and similarly a reduction factor $\sigma_X = 0.25$, $X \in \{I, A, T\}$ for the parasitoids and hypeparasitoids, according to their average two week-developmental period. With n denoting the week in the year, the actual implementation of the model relies on using (2.3), (2.10) in (2.17) and thus ultimately on the following equations,

$$\begin{aligned} I_{n+1} &= I_n + \sigma_I s_C E_{I,n-1} C_{n-2} - b_I I_n^2 - m_I I_n, \\ A_{n+1} &= A_n + \sigma_A s_C E_{A,n-1} C_{n-1} - b_A A_n^2 - m_A A_n, \\ T_{n+1} &= T_n + \sigma_T s_C E_{T,n-1} C_{n-1} - b_T T_n^2 - m_T T_n, \\ C_{n+1} &= C_n + \sigma_C s_C E_{C,n-3} C_{n-3} - b_C C_n^2 - m_C C_n. \end{aligned} \tag{4.3}$$

4.1. H. halys simulations

In Figure 3, left frame, we show the population behavior for the *H. halys* at the start of the simulations, in the year 2017. After use of the Matlab minimization routine fminsearch, the value of the whole overwintering population is 550.

For the following years, the optimization procedure gives the results of Table 13.

Table 13. Optimal intraspecific competition coefficients for *H. halys*.

year	2018	2019	2020	2021
b_C	0.092231	0.0036358	0.66779	0.0001896

4.2. Simulations for all the populations

For the simulations in the following years the values of the intraspecific coefficients for the other insects are taken to be equal to those of b_C that can be read for each year in Table 13, thus in each case

$$b_I = b_A = b_T = b_C.$$

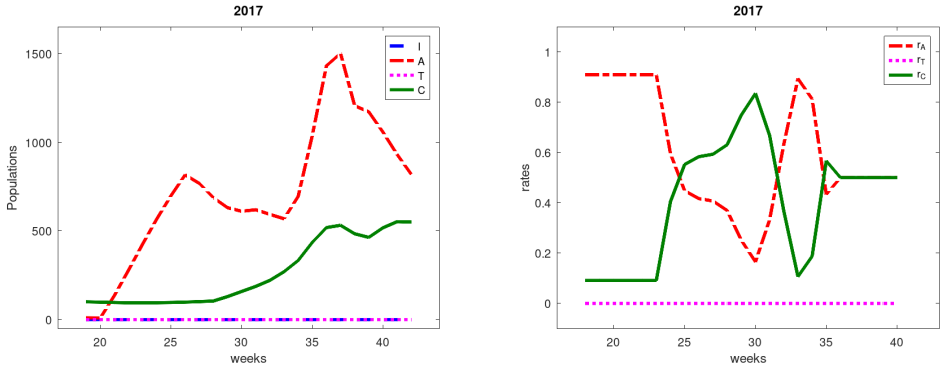

Figure 3. Left: populations simulations of the hyperparasitoid I, indigenous parasitoid A, exotic parasitoids T, and *H. halys* C in 2017; Right: the reproduction rates r_A of A, r_T of T, r_C of C in 2017.

The initial conditions for the year 2017 are given in (4.1). The results are shown in Figures 3–7, left frames.

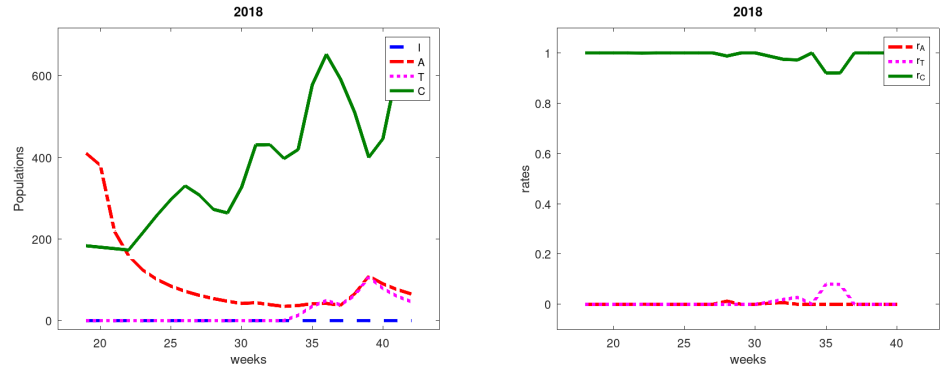

Figure 4. Left: populations simulations of the hyperparasitoid I, indigenous parasitoid A, exotic parasitoids T, and *H. halys* C in 2018; Right: the reproduction rates r_A of A, r_T of T, r_C of C in 2018.

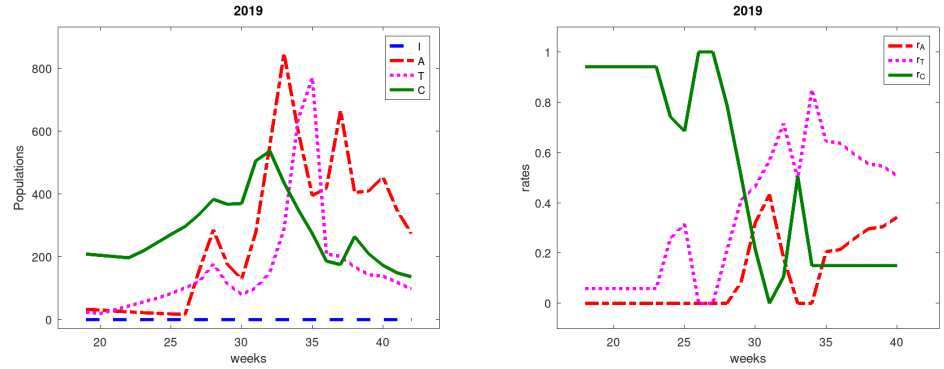

Figure 5. Left: populations simulations of the hyperparasitoid I, indigenous parasitoid A, exotic parasitoids T, and *H. halys* C in 2019; Right: the reproduction rates r_A of A, r_T of T, r_C of C in 2019.

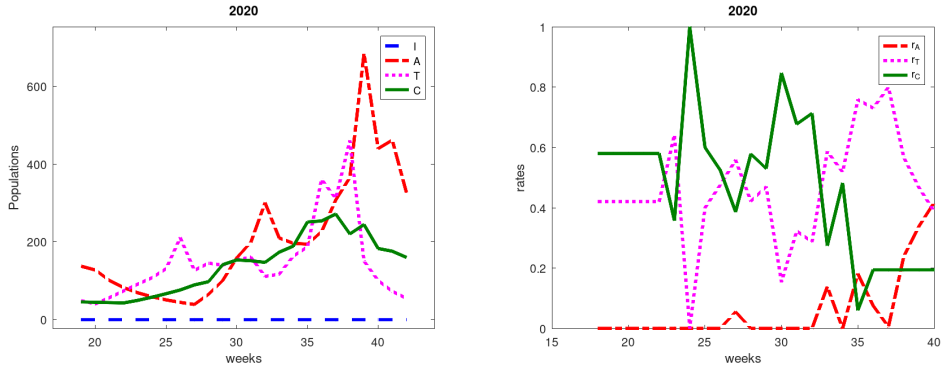

Figure 6. Left: populations simulations of the hyperparasitoid I, indigenous parasitoid A, exotic parasitoids T, and *H. halys* C in 2020; Right: the reproduction rates r_A of A, r_T of T, r_C of C in 2020.

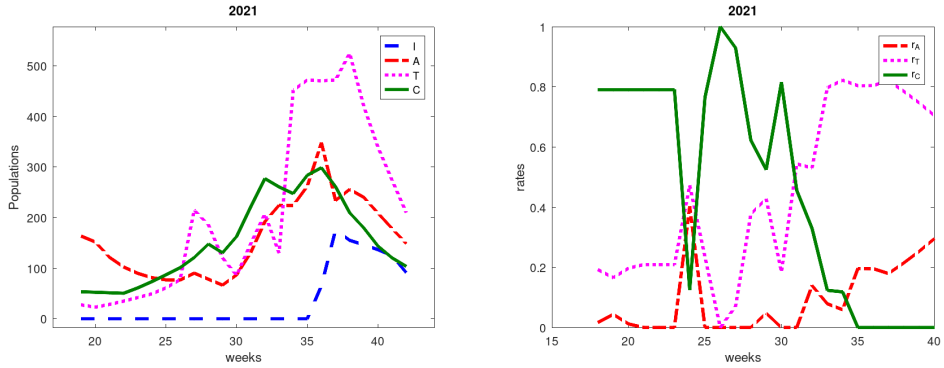

Figure 7. Left: populations simulations of the hyperparasitoid I, indigenous parasitoid A, exotic parasitoids T, and *H. halys* C in 2021; Right: the reproduction rates r_A of A, r_T of T, r_C of C in 2021.

4.3. Simulations for the reproduction rates

In view of the fact that the reproduction rates (2.3) and (2.4) are implicitly time-dependent, because they depend on the respective population sizes, it is worth investigating also how they behave, when the populations evolve in time. Figures 3–7, right frames, contain the results of the simulations.

4.4. Simulations discussion

The model simulations aim at a description of the *H. halys* invasion phenomenon. This species after its appearance, is monitored in the graphs starting from the year 2017 together with its indigenous parasitoid *A. bifasciatus*. In the following years the exotic parasitoids also appear and their joint action helps in keeping in check and finally curbing the *H. halys* population toward the end of the season. Indeed, in the first two years, the curve of the *H. halys* raises up, although not necessarily monotonically, from the spring to the fall.

In 2017, the *A. bifasciatus* experiences two peaks in the season, at the end of the spring or early summer, and toward the beginning of the fall.

In 2018, instead, it shows a declining behavior, compensated however by a raise in the *Trissolcus*

spp. population. The two together help in a sharp decline of the stink bug around the 40th week of the simulation, followed, however, by a further rise at the end of the season.

In 2019, *H. halys* attains a small peak in the spring and a much higher one in the summer, which are immediately followed by corresponding maxima of *A. bifasciatus*. In the second part of the summer, *Trissolcus* spp. also raises up to replace the indigenous parasitoid as the most effective control measure. Two other smaller maxima for both the pest and *A. bifasciatus* appear before the end of the season, driving the stink bug to lower values. The maximum for *H. halys* is a bit reduced with respect to the maximal value attained in 2018, being respectively slightly below and above 600.

In 2020, the *H. halys* population raises up almost monotonically until the end of the summer, but with values that are much below those of the previous year. This is due to the joint action of *A. bifasciatus* and *Trissolcus* spp., which grow and exhibit interlaced maxima, finding their maximum values at the beginning of the fall. Note that the *H. halys* population maximum, about 250, is halved with respect to the same value in 2019.

In 2021, a similar trend is shown by the model, only in part mimicking the previous year. Indeed now the hyperparasitoid emerges at the end of the summer, and at the same time, a reduction in the maximum value of *A. bifasciatus* and an increase in *Trissolcus* spp. in its place can be observed. The latter is the most effective control on the stink bug at the end of the season. The joint action of the three parasitoids curbs the final value of *H. halys* to half the final value that it attains in 2020, namely roughly 100 versus 200, in spite of the fact that the stink bug has an overall maximum 300 in the whole season that is higher than the corresponding one observed in the previous year, i.e., 250.

As a general remark, we can conclude that the simultaneous action of the three biological control mechanisms appears to be able to keep the invaders population down at the end of the simulations and at the end of the season.

5. System's equilibria

Here we summarize the results for which the mathematical details are provided in the Appendix A, both for the full model and in case of constant reproduction rates.

5.1. The full model

For the full model (2.17) with population-dependent reproduction rates, (A.1), in addition to the origin O and coexistence X_6, the other equilibria are found as follows, where the notation X_k with $X \in \{I, A, T\}$ emphasizes the value of the population X at the equilibrium E_k, $k = 1, \dots, 5$.

$$X_1 = (0, 0, 0, C_1), \quad C_1 = \frac{\sigma_C s_C E - m_C}{b_C}, \quad X_2 = (0, 0, T_2, C_2),$$
$$X_3 = (0, A_3, 0, C_3), \quad X_4 = (0, A_4, T_4, C_4), \quad X_5 = (I_5, 0, T_5, C_5).$$

Some of these equilibria cannot be determined analytically. However, for X_2 and X_3 some sufficient conditions for their feasible existence can be assessed.

Proposition 1. The origin is always feasible. If $m_I, m_A, m_T \neq 1$, O is locally asymptotically stable for

$$0 \leq E < \frac{m_C + 1}{\sigma_C s_C}. \tag{5.1}$$

Note that in general E represents the number of eggs in an egg mass from which individuals emerge. In fields data, generally it is found that $E \geq 3$, so that the origin is unstable in most of the cases.

Proposition 2. X_1 is feasible whenever

$$\sigma_C s_C E \geq m_C. \tag{5.2}$$

It is locally asymptotically stable if the following conditions are satisfied

$$\left|\frac{\sigma_A s_A \beta_A \sigma_C s_C E C_1}{q_{A,C}}\left[1+\frac{\sigma_T s_T \beta_T}{q_T}\right]-m_A\right|<1, \tag{5.3}$$
$$\left|\frac{\sigma_C s_C E C_1 \beta_T \sigma_T s_T}{q_T}-m_T\right|<1, \quad 0 \leq E < \frac{m_C+1}{\sigma_C s_C}.$$

Proposition 3. Sufficient conditions for the feasibility of X_2 are

$$E \geq \frac{1}{2\sigma_C s_C}\left[m_C+\sqrt{m_C^2+4\frac{b_C q_T m_T}{\sigma_C s_C \sigma_T s_T \beta_T}}\right]. \tag{5.4}$$

Corollary If (5.4) holds, we also have the constraint for the C population:

$$\frac{m_T q_T}{\sigma_C s_C \sigma_T s_T E \beta_T} \leq C_2 \leq \frac{\sigma_C s_C E - m_C}{b_C}.$$

Proposition 4. Letting

$$\Delta_{X_2} = [J_{33}(X_2) - J_{44}(X_2)]^2 - 4J_{34}(X_2)J_{43}(X_2),$$

the stability conditions for X_2 are

$$\left|\frac{\beta_T \beta_I \sigma_C s_C \sigma_I s_I \sigma_T s_T E C T}{(q_T+\sigma_T s_T T)\, q_I}-m_I\right|<1, \tag{5.5}$$
$$\left|\frac{\sigma_A s_A \beta_A \sigma_C s_C E C}{q_{A,C}}\left[1+\frac{\sigma_T s_T \beta_T}{(q_T+\sigma_T s_T T)}\right]-m_A\right|<1,$$
$$\left|J_{33}(X_2)+J_{44}(X_2) \pm \sqrt{\Delta_{X_2}}\right|<2.$$

Proposition 5. Sufficient conditions for the feasibility of X_3 are

$$E \geq \frac{1}{2\sigma_C s_C}\left[m_C+\sqrt{m_C^2+4\frac{b_C q_{A,C} m_A}{\sigma_A s_A \sigma_C s_C \beta_A}}\right], \tag{5.6}$$

Corollary Proposition 5 gives also the following constraint for the C population

$$\frac{m_A q_{A,C}}{\sigma_A s_A \sigma_C s_C E\, \beta_A} \leq C_3 \leq \frac{\sigma_C s_C E - m_C}{b_C}.$$

Proposition 6. X_3 is locally asymptotically stable if

$$|m_I|<1, \quad \left|\frac{\sigma_C s_C E C \beta_T \sigma_T s_T}{q_T}\left[1-\frac{\beta_A \sigma_A s_A A}{q_{A,T}+\sigma_A s_A A}\right]-m_T\right|<1, \tag{5.7}$$
$$\left|J_{22}(X_3)+J_{44}(X_3) \pm \sqrt{\Delta_{X_3}}\right|<2, \tag{5.8}$$

where

$$\Delta_{X_3} = [J_{22}(X_3) - J_{44}(X_3)]^2 - 4J_{24}(X_3)J_{42}(X_3).$$

5.2. A particular case

In the particular case of (2.17) with constant rates

$$r_A(A) = r_A, \quad r_T(T) = r_T, \quad h_I(I) = h_I, \quad h_A(A) = h_A. \tag{5.9}$$

equilibria are the origin, unconditionally feasible, and the coexistence point.

Proposition 7. Assuming (5.9), coexistence is given by

$$W = (I_+, A_+, T_+, C_+), \quad C_+ = \frac{1}{b_C}[\sigma_C s_C E(1 - r_A - r_T) - m_C], \tag{5.10}$$

where

$$I_+ = \frac{1}{2b_I}\left[-m_I + \sqrt{m_I^2 + 4b_I\sigma_I s_C E C_+ r_T h_I}\right],$$
$$A_+ = \frac{1}{2b_A}\left[-m_A + \sqrt{m_A^2 + 4b_A\sigma_A s_C E C_+ [r_A + r_T h_A]}\right],$$
$$T_+ = \frac{1}{2b_T}\left[-m_T + \sqrt{m_T^2 + 4b_T\sigma_T s_C E C_+ r_T(1 - h_A - h_I)}\right].$$

and for its feasibility we have the constraint

$$E > \frac{m_C}{\sigma_C s_C (1 - r_A - r_T)}. \tag{5.11}$$

Proposition 8. Assuming (5.9), the origin is locally asymptotically stable for the following alternatives:

- Assuming that $m_X \in [0, 1)$, $X \in \{I, A, T\}$ and $r_A + r_T < 1$, O is asymptotically stable if and only if

$$0 \le E < \frac{m_C + 1}{\sigma_C s_C (1 - r_A - r_T)}; \tag{5.12}$$

- If $m_{\widehat{X}} = 1$, for some $\widehat{X} \in \{I, A, T\}$, while $m_X \in [0, 1)$ for $X \in \{I, A, T\} - \{\widehat{X}\}$, and (5.12) holds, O is stable, but not asymptotically.

Proposition 9. Assuming (5.9), using the feasibility condition, (5.11), and (5.10) local asymptotic stability is guaranteed by the following sets of inequalities, for $X \in \{I, A, T\}$:

$$E \in [0, \zeta_{X+}), \quad E < \frac{m_C + 1}{\sigma_C s_C (1 - r_A - r_T)}, \tag{5.13}$$

where, using (A.6)

$$\zeta_{X\pm} = \frac{m_C}{2\sigma_C s_C (1 - r_A - r_T)} \pm \frac{\sqrt{m_C^2 + \gamma_X b_C (1 - r_A - r_T)}}{2\sigma_C s_C (1 - r_A - r_T)}.$$

6. Conclusions

In this work, we modeled the parasitism and hyperparasitism on *H. halys* eggs in North Italy using both data collected during a five-year field survey and data available in the literature. The model presented here is of descriptive nature, although, as stated above, clearly based on a sound ecological basis. It cannot be taken as a tool for forecasts, because it is still in a rudimentary phase and therefore validation with real data at this stage is not considered. We plan in the future to refine and validate it accordingly.

As all models, the one considered here is subject to several limiting assumptions, listed below.

- In the modeling procedure juvenile stages do not appear explicitly; however insects experience developmental stages that differ for heterometabolous, (i.e., *H. halys*), and holometabolous, (i.e., parasitoids and hyperparasitoid) during their evolution from egg to adulthood.
- To fit the gaps on the egg masses data, an interpolation procedure was used in which eggs are forced to disappear at the start and end of each year.
- Unlike field insect data, i.e., field collected eggs and trap catch counts, biological parameters, such as longevity and sex ratio, came from laboratory experiments, which may differ from those occurring in the field.
- Population data are just estimates on the actual numbers of individuals in the environment; they are obtained as averages of insects captured at various sites, differing greatly for environmental conditions. This applies to *H. halys* as well as to parasitoids, counted as averages of those emerging from field collected eggs.
- All populations at the start of the following year come from the corresponding values at the end of the fall of the current year, discounted by a fixed fraction representing their mortality during overwintering, which is arbitrarily taken for the whole parasitoid populations. However, climatic conditions may change, so that the assumption of constant winter mortality could be refined.
- Intraspecific competition rates are not measurable in the field. Thus b_I, b_A and b_T are set to the same value b_C that is instead calculated for *H. halys* through least squares regression, see Section 4.
- The average lifetime of the indigenous parasitoid is set to 14 weeks while A hyperparasitizes C within the first 3 days.
- Not having data at the start of 2017, the value of the *H. halys* is taken to be of the same order of the one assessed by traps in the following years, while for A we set a smaller hypothetical value than the one for *H. halys*, since only a fraction of A parasitizes C (4.1).

The model equilibria have been analytically assessed, when possible. Ecosystem collapse, represented by the origin, could occur in case of population-dependent reproduction rates if condition (5.1) holds. In general however, it does not, as the number of eggs in an egg mass usually exceeds the critical value 3.

H. halys alone can stably survive at equilibrium X_1, if feasibility (5.2) holds and conditions (5.3) are satisfied.

For both the points with *H. halys* and just one of the parasitoids T or A we have obtained sufficient conditions for their feasibility, (5.4) and (5.6). They are not stringent in the sense that even in case they are violated, these equilibria could nevertheless exist. Their local asymptotic stability conditions have

instead completely assessed, respectively by (5.5) for X_2 and the equations (5.7) and (5.8) for X_3. An explicit interpretation of their meanings in terms of the model parameters appears however to be very difficult.

The coexistence point and the equilibrium with no hyperparasitoid I lead to nonlinear algebraic systems for which the analytic solution is not available. Similarly, the Jacobian evaluated at these points leads to a fourth order matrix, whose eigenvalues are impossible to calculate; formally, we could write the Routh-Hurwitz conditions for stability, but they would hardly shed any light on this issue. The recourse to numerical methods is therefore imperative.

In our simulations the populations of the indigenous and generalist parasitoid, *A. bifasciatus*, fluctuated over the five years, confirming that this species alone cannot significantly suppress *H. halys* populations, consistent with what was observed in previous field trials [9, 33]. Examples of failed biological control exist in the literature. The most notable case concerns aphid species in open-air crops, both horticultural and fruit with the use of parasitoid species and the role played by hyperparasitoid species; both experimental [34] and by the use of mathematical models [35]. However, we are not observing a failure of biological control due to hyperparasitoid activity but merely describing the situation that, in our opinion, has not yet reached an equilibrium. Instead, populations of the exotic parasitoids *T. japonicus* and *T. mitsukurii* increased greatly from 2019 to 2021, after they first appeared in 2018 and 2016 respectively. This led to *H. halys* populations gradually decreasing, demonstrating that the exotic species can have a strong impact on their host. The hyperparasitoid *A. sinicus*, which in these surveys was detected for the first time in 2020, even if it had already been detected starting from 2016 in the study area, the Piedmont region [9], did not show as large an increase in the following years as the two *Trissolcus* species, thus demonstrating a minimal impact on parasitoids, without hampering their activity on bug populations, as modeled in [36]. Certainly, egg parasitoids are not the only natural enemies of *H. halys*. Indeed, eggs are also attacked by predators [33, 37], and mobile stages can be affected by other parasitoids, predators, and entomopathogens [38, 39]. Egg parasitoids clearly do not, by themselves, suppress *H. halys* populations to noneconomic levels, as already modeled in [36], but can play an important role in reducing *H. halys* populations, as seen in these simulations and also by [36]. These interactions between host, parasitoids, and hyperparasitoids tend to reach different equilibria over time, especially as the populations adapt to environmental pressures. In our model, this is reflected in the fluctuating dynamics of *A. bifasciatus* and the stabilizing effect of *T. japonicus* and *T. mitsukurii* on *H. halys* populations. The stability and biological significance of these equilibria depend on multiple factors, such as the reproductive rates of the species and their susceptibility to predation or parasitism, which our model attempts to approximate. More extensive field data could improve our understanding of these equilibria and the conditions that favor stability or instability in these populations. However, our simulations are based on partial field observations, as adults and eggs were not sampled at the same sites, and parameters from literature were obtained from laboratory trials. Furthermore, climate conditions, and climate change, were not considered, but they can affect populations of both host and parasitoids [40–45]. Incorporating these additional variables could further describe the stability of the modeled interactions and the long-term biological significance of these parasitoid-host dynamics. More accurate simulations could be made with additional collection of field data, and also by adding climatic data in the model.

Use of AI tools declaration

The authors declare they have not used Artificial Intelligence (AI) tools in the creation of this article.

Conflict of interest

The authors declare there is no conflict of interest.

Acknowledgments

The authors are very much indebted to the referees for their careful work that considerably helped in the improvement of the paper.

References

1. T. C. Leskey, A. L. Nielsen, Impact of the invasive brown marmorated stink bug in North America and Europe: history, biology, ecology, and management, *Annu. Rev. Entomol.*, **63** (2018), 599–618. https://doi.org/10.1146/annurev-ento-020117-043226
2. F. Cianferoni, F. Graziani, P. Dioli, F. Ceccolini, Review of the occurrence of *Halyomorpha halys* (Hemiptera: Heteroptera: Pentatomidae) in Italy, with an update of its European and World distribution, *Biologia*, **73** (2018), 599–607. https://doi.org/10.2478/s11756-018-0067-9
3. F. Cianferoni, F. Graziani, F. Ceccolini, The unstoppable march of *Halyomorpha halys*: new first country records (Hemiptera, Pentatomidae), *Spixiana*, **42** (2019), 60.
4. M. Cesari, L. Maistrello, F. Ganzerli, P. Dioli, L. Rebecchi, R. Guidetti, A pest alien invasion in progress: potential pathways of origin of the brown marmorated stink bug *Halyomorpha halys* populations in Italy, *J. Pest Sci.*, **88** (2015), 1–7. https://doi.org/10.1007/s10340-014-0634-y
5. L. Bosco, S. T. Moraglio, L. Tavella, *Halyomorpha halys*, a serious threat for hazelnut in newly invaded areas, *J. Pest Sci.*, **91** (2018), 661–670. https://doi.org/10.3390/insects11120866
6. E. Costi, T. Haye, L. Maistrello, . Biological parameters of the invasive brown marmorated stink bug, *Halyomorpha halys*, in southern Europe, *J. Pest Sci.*, **90** (2017), 1059–1067. https://doi.org/10.1007/s10340-017-0899-z
7. N. Mills, Parasitoids, in *Encyclopedia of insects*, Academic Press, (2009), 748–751.
8. J. M. Stahl, D. Babendreier, C. Marazzi, S. Caruso, E. Costi, L. Maistrello, et al., Can *Anastatus bifasciatus* be used for augmentative biological control of the brown marmorated stink bug in fruit orchards?, *Insects*, **10** (2019), 108. https://doi.org/10.3390/insects10040108
9. S. T. Moraglio, F. Tortorici, M. G. Pansa, G. Castelli, M. Pontini, S. Scovero, et al., A 3-year survey on parasitism of *Halyomorpha halys* by egg parasitoids in Northern Italy, *J. Pest Sci.*, **93** (2020), 183–194. https://doi.org/10.1007/s10340-019-01136-2
10. J. Zhang, F. Zhang, T. Gariepy, P. Mason, D. Gillespie, E. Talamas, et al., Seasonal parasitism and host specificity of *Trissolcus japonicus* in Northern China, *J. Pest Sci.*, **90** (2017), 1127–1141. https://doi.org/10.1007/s10340-017-0863-y

11. M. T. Kamiyama, K. Matsuura, T. Hata, T. Yoshimura, C. C. S. Yang, Seasonal parasitism of native egg parasitoids of brown marmorated stink bug (*Halyomorpha halys*) in Japan, *J. Pest Sci.*, **95** (2022), 1067–1079. https://doi.org/10.1007/s10340-021-01455-3
12. J. R. Lara, C. H. Pickett, M. T. Kamiyama, S. Figueroa, M. Romo, C. Cabanas, et al., Physiological host range of *Trissolcus japonicus* in relation to *Halyomorpha halys* and other pentatomids from California, *BioControl*, **64** (2019), 513–528. https://doi.org/10.1007/s10526-019-09950-4
13. T. Haye, S. T. Moraglio, J. Stahl, S. Visentin, T. Gregorio, L. Tavella, Fundamental host range of *Trissolcus japonicus* in Europe, *J. Pest Sci.*, **93** (2020), 171–182. https://doi.org/10.1007/s10340-019-01127-3
14. G. Sabbatini-Peverieri, L. Boncompagni, G. Mazza, F. Paoli, L. Dapporto, L. Giovannini, et al., Combining physiological host range, behavior and host characteristics for predictive risk analysis of *Trissolcus japonicus*, *J. Pest Sci.*, **94** (2021), 1003–1016. https://doi.org/10.1007/s10340-020-01311-w
15. G. Sabbatini Peverieri, E. Talamas, M. C. Bon, L. Marianelli, I. Bernardinelli, G. Malossini, et al., Two asian egg parasitoids of *Halyomorpha halys* (Stål) (Hemiptera, Pentatomidae) emerge in Northern Italy: *Trissolcus mitsukurii* (Ashmead) and *Trissolcus japonicus* (Ashmead) (Hymenoptera, Scelionidae), *J. Hymen. Res.*, **67** (2018), 37–53. https://doi.org/10.3897/jhr.67.30883
16. D. Scaccini, M. Falagiarda, F. Tortorici, I. Martinez-Sañudo, P. Tirello, Y. Reyes-Domínguez, et al., An insight into the role of *Trissolcus mitsukurii* as biological control agent of *Halyomorpha halys* in Northeastern Italy, *Insects*, **11** (2020), 306. https://doi.org/10.3390/insects11050306
17. L. Giovannini, G. Sabbatini-Peverieri, L. Marianelli, G. Rondoni, E. Conti, P. F. Roversi, Physiological host range of *Trissolcus mitsukurii*, a candidate biological control agent of *Halyomorpha halys* in Europe, *J. Pest Sci.*, **95** (2022), 605-–618. https://doi.org/10.1007/s10340-021-01415-x
18. L. Zapponi, F. Tortorici, G. Anfora, S. Bardella, M. Bariselli, L. Benvenuto, et al., Assessing the distribution of exotic egg parasitoids of *Halyomorpha halys* in Europe with a large-scale monitoring program, *Insects*, **12** (2021), 316. https://doi.org/10.3390/insects12040316
19. J. K. Konopka, T. Haye, T. D. Gariepy, J. N. McNeil, Possible coexistence of native and exotic parasitoids and their impact on control of *Halyomorpha halys*, *J. Pest Sci.*, **90** (2017), 1119–1125. https://doi.org/10.1007/s10340-017-0851-2
20. G. Sabbatini-Peverieri, M. D. Mitroiu, M. C. Bon, R. Balusu, L. Benvenuto, I. Bernardinelli, et al., Surveys of stink bug egg parasitism in Asia, Europe and North America, morphological taxonomy, and molecular analysis reveal the Holarctic distribution of *Acroclisoides sinicus* (Huang and Liao) (Hymenoptera, Pteromalidae), *J. Hymen. Res.*, **74** (2019), 123–151. https://doi.org/10.3897/jhr.74.46701
21. A. Mele, D. Scaccini, A. Pozzebon, Hyperparasitism of *Acroclisoides sinicus* (Huang and Liao) (Hymenoptera: Pteromalidae) on two biological control agents of *Halyomorpha halys*, *Insects*, **12** (2021), 617. https://doi.org/10.3390/insects12070617

22. D. J. Sullivan, Hyperparasitism, in *Encyclopedia of insects*, Academic Press, (2009), 486–488.

23. G. Sabbatini-Peverieri, C. Dieckhoff, L. Giovannini, L. Marianelli, P. F. Roversi, K. Hoelmer, Rearing *Trissolcus japonicus* and *Trissolcus mitsukurii* for biological control of *Halyomorpha halys*, *Insects*, **11** (2020), 787. https://doi.org/10.3390/insects11110787

24. B. N. Govindan, W. D. Hutchison, Influence of temperature on age-stage, two-sex life tables for a Minnesota-acclimated population of the brown marmorated stink bug (*Halyomorpha halys*), *Insects*, **11** (2020), 108. https://doi.org/10.3390/insects11020108

25. J. M. Stahl, D. Babendreier, T. Haye, Using the egg parasitoid *Anastatus bifasciatus* against the invasive brown marmorated stink bug in Europe: can non-target effects be ruled out?, *J. Pest Sci.*, **91** (2018), 1005–1017. https://doi.org/10.1007/s10340-018-0969-x

26. D. M. Lowenstein, H. Andrews, R. J. Hilton, C. Kaiser, N. G. Wiman, Establishment in an introduced range: dispersal capacity and winter survival of *Trissolcus japonicus*, an adventive egg parasitoid, *Insects*, **10** (2019), 443. https://doi.org/10.3390/insects10120443

27. L. Giovannini, G. Sabbatini-Peverieri, P. G. Tillman, K. A. Hoelmer, P. F. Roversi, Reproductive and developmental biology of *Acroclisoides sinicus*, a hyperparasitoid of scelionid parasitoids, *Biology*, **10** (2021), 229. https://doi.org/10.3390/biology10030229

28. J. M. Stahl, D. Babendreier, T. Haye, Life history of *Anastatus bifasciatus*, a potential biological control agent of the brown marmorated stink bug in Europe, *Biol. Control*, **129** (2019), 178–186. https://doi.org/10.1016/j.biocontrol.2018.10.016

29. R. Arakawa, M. Miura, M. Fujita, Effects of host species on the body size, fecundity, and longevity of *Trissolcus mitsukurii* (Hymenoptera: Scelionidae), a solitary egg parasitoid of stink bugs, *Appl. Entomol. Zool.*, **39** (2004), 177–181. https://doi.org/10.1303/aez.2004.177

30. H. R. McIntosh, V. P. Skillman, G. Galindo, J. C. Lee, Floral Resources for *Trissolcus japonicus*, a Parasitoid of *Halyomorpha halys*. *Insects*, **11** (2020), 413. https://doi.org/10.3390/insects11070413

31. M. Rot, L. Maistrello, E. Costi, S. Trdan, Biological parameters, phenology and temperature requirements of *Halyomorpha halys* (Hemiptera: Pentatomidae) in the Sub-Mediterranean climate of Western Slovenia, *Insects*, **13** (2022), 956. https://doi.org/10.3390/insects13100956

32. T. Haye, S. Abdallah, T. Gariepy, D. Wyniger, Phenology, life table analysis and temperature requirements of the invasive brown marmorated stink bug, *Halyomorpha halys*, in Europe, *J. Pest Sci.*, **87** (2014), 407–418. https://doi.org/10.1007/s10340-014-0560-z

33. E. Costi, T. Haye, L. Maistrello, Surveying native egg parasitoids and predators of the invasive *Halyomorpha halys* in Northern Italy, *J. Appl. Entomol.*, **143** (2019), 299–307. https://doi.org/10.1111/jen.12590

34. D. J. Sullivan, Insect hyperparasitism, *Ann. Rev. Entomol.*, **32** (1987), 49–70.

35. M. R. Nematollahi, Y. Fathipour, A. A. Talebi, J. Karimzadeh, M. P. Zalucki, Parasitoid- and Hyperparasitoid-Mediated seasonal dynamics of the cabbage aphid (Hemiptera: Aphididae), *Environ. Entomol.*, **43** (2014), 1542–1551. https://doi.org/10.1603/EN14155

36. A. P. Gutierrez, G. Sabbatini Peverieri, L. Ponti, L. Giovannini, P. F. Roversi, A. Mele, et al., Tritrophic analysis of the prospective biological control of brown marmorated stink bug, *Halyomorpha halys*, under extant weather and climate change, *J. Pest Sci.*, **96** (2023), 921–942. https://doi.org/10.1007/s10340-023-01610-y

37. W. R. Morrison III, B. R. Blaauw, A. L. Nielsen, E. Talamas, T. C. Leskey, Predation and parasitism by native and exotic natural enemies of *Halyomorpha halys* (Stål) (Hemiptera: Pentatomidae) eggs augmented with semiochemicals and differing host stimuli. *Biol. Control*, **121** (2018), 140–150. https://doi.org/10.1016/j.biocontrol.2018.02.016

38. G. Bulgarini, Z. Badra, S. Leonardi, L. Maistrello, Predatory ability of generalist predators on eggs, young nymphs and adults of the invasive *Halyomorpha halys* in southern Europe, *BioControl*, **66** (2021), 355–366. https://doi.org/10.1007/s10526-020-10066-3

39. D. H. Lee, B. D. Short, S. V. Joseph, J. C. Bergh, T. C. Leskey, Review of the biology, ecology, and management of *Halyomorpha halys* (Hemiptera: Pentatomidae) in China, Japan, and the Republic of Korea, *Environ. Entomol.*, **42** (2013), 627–641. https://doi.org/10.1603/EN13006

40. G. A. Avila, J. G. Charles, Modelling the potential geographic distribution of *Trissolcus japonicus*: a biological control agent of the brown marmorated stink bug, Halyomorpha halys, *BioControl*, **63** (2018), 505–518. https://doi.org/10.1007/s10526-018-9866-8

41. D. J. Kriticos, J. M. Kean, C. B. Phillips, S. D. Senay, H. Acosta, T. Haye, The potential global distribution of the brown marmorated stink bug, *Halyomorpha halys*, a critical threat to plant biosecurity, *J. Pest Sci.*, **90** (2017), 1033–1043. https://doi.org/10.1007/s10340-017-0869-5

42. S. Stoeckli, R. Felber, T. Haye, Current distribution and voltinism of the brown marmorated stink bug, *Halyomorpha halys*, in Switzerland and its response to climate change using a high-resolution CLIMEX model, International Journal of Biometeorology, **64** (2020), 2019–2032. https://doi.org/10.1007/s00484-020-01992-z

43. T. Yonow, D. J. Kriticos, N. Ota, G. A. Avila, K. A. Hoelmer, H. Chen, et al., Modelling the potential geographic distribution of two *Trissolcus* species for the brown marmorated stink bug, *Halyomorpha halys*, *Insects*, **12** (2021), 491. https://doi.org/10.3390/insects12060491

44. F. Tortorici, P. Bombi, L. Loru, A. Mele, S. T. Moraglio, D. Scaccini, et al., *Halyomorpha halys* and its egg parasitoids *Trissolcus japonicus* and *T. mitsukurii*: the geographic dimension of the interaction, *NeoBiota*, **85** (2023), 197–221. https://doi.org/10.3897/neobiota.85.102501

45. A. Mele, D. S. Avanigadda, E. Ceccato, G. B. Olawuyi, F. Simoni, C. Duso, et al., Comparative life tables of *Trissolcus japonicus* and *Trissolcus mitsukurii*, egg parasitoids of *Halyomorpha halys*, *Biol. Control*, **195** (2024), 105548.

Appendix

A. Mathematical appendix: Equilibria analysis of the full model

In this situation, (2.17) has population-dependent reproduction rates,

$$r_X = r_X(X), \quad X \in \{A, T\}. \tag{A.1}$$

In addition to the origin O and coexistence X_6, the other equilibria are found as follows.

$$X_1 = (0, 0, 0, C_1), \quad C_1 = \frac{\sigma_C s_C E - m_C}{b_C}, \quad X_2 = (0, 0, T_2, C_2),$$
$$X_3 = (0, A_3, 0, C_3), \quad X_4 = (0, A_4, T_4, C_4), \quad X_5 = (I_5, 0, T_5, C_5).$$

Some of these equilibria cannot be determined analytically. However, for X_2 and X_3 some sufficient conditions for their feasible existence can be assessed.

A.1. Feasibility

A.1.1. Equilibrium X_2

Proof of Proposition 3

For X_2, observing that $C \neq 0$, $T \neq 0$, the equilibrium equations of (2.17) to be considered are the last two. They can be rearranged as follows:

$$C = \Pi(T) = \frac{1}{\sigma_C s_C s_T E \beta_T}[\sigma_T s_T b_T T^2 + (\sigma_T s_T m_T + b_T q_T)T + m_T q_T] \tag{A.2}$$
$$C = \Phi(T) = \frac{1}{b_C}\left[\sigma_C s_C E - m_C - \frac{\sigma_C s_C \sigma_T s_T E \beta_T T}{q_T + \sigma_T s_T T}\right]$$

where $\Pi(T)$ is a convex parabola in the $T - C$ plane through the point on the vertical axis

$$\left(0, \frac{m_T q_T}{\sigma_C s_C \sigma_T s_T E \beta_T}\right)$$

where it has a positive slope and $\Phi(T)$ is a hyperbola with intercept at the origin

$$\left(0, \frac{\sigma_C s_C E - m_C}{b_C}\right).$$

and horizontal asymptote with height $b_C^{-1}[\sigma_C s_C E(1 - \beta_T) - m_C]$. Note that $\Phi(T)$ is always decreasing, since

$$\frac{d\Phi(T)}{dT} = -\frac{\sigma_C s_C \sigma_T s_T E \beta_T q_T}{(q_T + \sigma_T s_T T)^2} < 0.$$

An intersection of $\Pi(T)$ and $\Phi(T)$ in the first quadrant is thus guaranteed if

$$\frac{m_T q_T}{\sigma_C s_C \sigma_T s_T E \beta_T} \leq \frac{\sigma_C s_C E - m_C}{b_C}$$

so that the sufficient condition in this case turns out to be (5.4).

A.1.2. Equilibrium X_3

Proof of Proposition 5

Here, we need to consider the second and fourth equilibrium equations of (2.17). Thus, we need to intersect the curves

$$C = \Psi(A) = \frac{1}{\sigma_A s_A \sigma_C s_C E \beta_A}\left[b_A \sigma_A s_A b_A A^2 + (b_A q_{A,C} + \sigma_A s_A m_A)A + m_A q_{A,C}\right], \tag{A.3}$$

$$C = \Phi(A) = \frac{1}{b_C}\left(\sigma_C s_C E - m_C - \frac{\sigma_A s_A \sigma_C s_C E \beta_A A}{q_{A,C} + \sigma_A s_A A}\right).$$

Again $\Psi(A)$ is a convex parabola and $\Psi(A)$ is a hyperbola in the $A - C$ plane, respectively through the points

$$\left(0, \frac{m_A q_{A,C}}{\sigma_C s_A \sigma_C s_C E\, \beta_A}\right), \quad \left(0, \frac{\sigma_C s_C E - m_C}{b_C}\right).$$

At the origin, the slope of $\Psi(A)$ is positive and the one of $\Phi(A)$ is negative. Thus an intersection exists if (5.6) holds.

A.2. Local Stability

In this section we recall the values of some important parameters, (4.2), that are used in the analysis that follows. System (2.17), in view now of the assumptions (A.1), has the following Jacobian $J = J_{ik}$, $i, k = 1, \ldots, 4$, with $J_{1,2} = J_{2,1} = J_{4,1} = 0$ and

$$J_{1,1} = \frac{\beta_T \beta_I q_I \sigma_C s_C \sigma_I s_I \sigma_T s_T ECT}{(q_T + \sigma_T s_T T)(q_I + \sigma_I s_I I)^2} - 2b_I I - m_I, \quad J_{1,3} = \frac{\sigma_C s_C \sigma_I s_I \sigma_T s_T \beta_T \beta_I q_T ECI}{(q_T + \sigma_T s_T T)^2 (q_I + \sigma_I s_I I)}, \tag{A.4}$$

$$J_{1,4} = \frac{\sigma_C s_C E \beta_T \beta_I \sigma_I s_I \sigma_T s_T TI}{(q_T + \sigma_T s_T T)(q_I + \sigma_I s_I I)}, \quad J_{2,4} = \sigma_C s_C E \frac{\beta_A \sigma_A s_A A}{q_{A,C} + \sigma_A s_A A}\left[1 + \frac{\beta_T \sigma_T s_T T}{q_T + \sigma_T s_T T}\right],$$

$$J_{2,2} = \frac{\sigma_A s_A q_{A,C} \beta_A \sigma_C s_C EC}{(q_{A,C} + \sigma_A s_A A)^2}\left[1 + \frac{\sigma_T s_T \beta_T}{q_T + \sigma_T s_T T}\right] - 2b_A A - m_A$$

$$J_{2,3} = \frac{\sigma_C s_C EC \beta_T \sigma_T s_T q_T \beta_A \sigma_A s_A A}{(q_T + \sigma_T s_T T)^2 (q_{A,T} + \sigma_A s_A A)}, \quad J_{3,1} = \frac{\sigma_C s_C EC \beta_T \sigma_T s_T T}{q_T + \sigma_T s_T T}\left[1 + \frac{\beta_I \sigma_I s_I q_I}{(q_I + \sigma_I s_I I)^2}\right],$$

$$J_{3,2} = \frac{\sigma_C s_C EC \beta_T \sigma_T s_T T}{q_T + \sigma_T s_T T}\left[1 + \frac{\beta_A \sigma_A s_A q_{A,T}}{(q_{A,T} + \sigma_A s_A A)^2}\right], \quad J_{4,2} = \frac{\sigma_C s_C EC \beta_A \sigma_A s_A q_{A,T}}{(q_{A,T} + \sigma_A s_A A)^2},$$

$$J_{3,3} = \frac{\sigma_C s_C EC \beta_T \sigma_T s_T q_T}{(q_T + \sigma_T s_T T)^2}\left[1 - \frac{\beta_A \sigma_A s_A A}{q_{A,T} + \sigma_A s_A A} - \frac{\beta_I \sigma_I s_I I}{q_I + \sigma_I s_I I}\right] - 2b_T T - m_T,$$

$$J_{3,4} = \frac{\sigma_C s_C E \beta_T \sigma_T s_T T}{q_T + \sigma_T s_T T}\left[1 - \frac{\beta_A \sigma_A s_A A}{q_{A,T} + \sigma_A s_A A} - \frac{\beta_I \sigma_I s_I I}{q_I + \sigma_I s_I I}\right] \quad J_{4,3} = \frac{\sigma_C s_C EC \beta_T \sigma_T s_T q_T}{(q_T + \sigma_T d s_T T)^2},$$

$$J_{4,4} = \sigma_C s_C E\left[1 - \frac{\beta_A \sigma_A s_A A}{q_{A,T} + \sigma_A s_A A} - \frac{\beta_I \sigma_I s_I I}{q_I + \sigma_I s_I I}\right] - 2b_C C - m_C.$$

A.2.1. Origin

Proof of Proposition 1

Here the eigenvalues of (A.4) are all explicitly known,

$$\lambda_1^O = -m_I, \quad \lambda_2^O = -m_A, \quad \lambda_3^O = -m_T, \quad \lambda_4^O = \sigma_C s_C E - m_C$$

thus yielding (5.1).

A.2.2. Equilibrium X_1

Proof of Proposition 2

Feasibility follows by imposing the nonnegativity of the C population at equilibrium, C_1, giving (5.2).

For stability, again the four eigenvalues are explicitly found. For $q_{A,C}, q_T \neq 0$, we have

$$\lambda_1^{X_1} = -m_I, \quad \lambda_2^{X_1} = \frac{\sigma_A s_A \beta_A \sigma_C s_C E C_1}{q_{A,C}} \left[1 + \frac{\sigma_T s_T \beta_T}{q_T}\right] - m_A,$$
$$\lambda_3^{X_1} = \frac{\sigma_C s_C E C_1 \beta_T \sigma_T s_T}{q_T} - m_T, \quad \lambda_4^{X_1} = m_C - \sigma_C s_C E = -b_C C_1 < 0,$$

from which (5.3) follows.

Remark 1 For $\beta_A = \beta_T = 0$, the second and third eigenvalues would coincide with the corresponding ones of the origin, and the analysis would then be identical to the one of O. The claim of Proposition 2 follows in view of the values of Table 1, $-1 \leq \lambda_1^{X_1} \leq 0$.

A.2.3. Equilibrium X_2

Proof of Proposition 4

In this case two eigenvalues are known immediately, $J_{11}^{X_2}$ and $J_{22}^{X_2}$, because the Jacobian factorizes, providing the first two conditions (5.5). The remaining two are obtained from the roots of the quadratic equation

$$\lambda^2 - (J_{33}(X_2) + J_{44}(X_2))\,\lambda + J_{33}(X_2)J_{44}(X_2) - J_{34}(X_2)J_{43}(X_2) = 0.$$

A.2.4. Equilibrium X_3

Proof of Proposition 6

Here again, the Jacobian factorizes giving two explicit eigenvalues $J_{11}^{X_3}$ and $J_{33}^{X_3}$, giving the first two stability conditions (5.7), while the other ones are the roots of the quadratic equation

$$\lambda^2 - (J_{22}(X_3) + J_{44}(X_3))\,\lambda + J_{22}(X_3)J_{44}(X_3) - J_{24}(X_3)J_{42}(X_3) = 0,$$

which provide the last two stability conditions, (5.8).

A.3. Analysis of a particular case

Proof of Proposition 7

We consider here the case where the primary parasitization rates r_A and r_T, as well as the hyperparasitizations h_I, h_A, are assumed to be constant, (5.9).

The feasible equilibria of the system (2.17) are just the origin O and coexistence W. The latter in principle is not unique, but only one instance can be accepted, (5.10).

Note that for feasibility of W we must impose that the C population is nonnegative, giving the constraint (5.11), with $1 - r_A - r_T > 0$ stemming from (2.10). Note that if (5.11) holds, $I_- \leq 0$, $A_- \leq 0$, $T_- \leq 0$ and the other equilibria are not feasible. Since $I_+ \geq 0$, $A_+ \geq 0$, $T_+ \geq 0$, the only feasible equilibria are the origin and W.

A.3.1. Stability

For the stability, we need the Jacobian of (2.17),

$$\widetilde{J} = \begin{bmatrix} -2b_I I - m_I & 0 & 0 & \sigma_I s_C E r_T h_I \\ 0 & -2b_A A - m_A & 0 & \sigma_A s_C E\,(r_A + r_T h_A) \\ 0 & 0 & -2b_T T - m_T & \sigma_T s_C E r_T\,(1 - h_A - h_I) \\ 0 & 0 & 0 & \widetilde{J}_{4,4} \end{bmatrix} \tag{A.5}$$

where

$$\widetilde{J}_{4,4} = \sigma_C s_C E\,(1 - r_A - r_T) - 2b_C C - m_C$$

Proof of Proposition 8

At the origin, the eigenvalues are easily determined, $\mu_1^O = -m_I$, $\mu_2^O = -m_A$, $\mu_3^O = -m_T$, $\mu_4^O = \sigma_C s_C E\,(1 - r_A - r_T) - m_C$. While the first three lie in $[-1, 0]$, for the fourth one there are the alternatives in the statement of Proposition 8. Note that if $r_A + r_T = 1$, then $\mu_4^O = -m_C$ and similar considerations apply here as well. We omit the details.

Proof of Proposition 9

For the stability of W, we have again four explicit eigenvalues for the Jacobian evaluated at this equilibrium:

$$\begin{aligned} \mu_1^W &= -\sqrt{m_I^2 + 4\sigma_I s_C E b_I r_T h_I C_+} < 0, \\ \mu_2^W &= -\sqrt{m_A^2 + 4\sigma_A s_C E b_A (r_A + r_T h_A) C_+} < 0, \\ \mu_3^W &= -\sqrt{m_T^2 + 4\sigma_T s_C E b_T r_T (1 - h_A - h_I) C_+} < 0, \\ \mu_4^W &= m_C - \sigma_C s_C E\,(1 - r_A - r_T)\,. \end{aligned}$$

From the feasibility of W, (5.11), we find that $\mu_4 < 0$. For the asymptotic stability of the coexistence equilibrium, we need $\mu_k^W \in (-1, 0)$, $k = 1, \ldots, 4$. If one of these inequalities attains the lower bound, only stability can be obtained. Once again, using (5.11) and (5.10) asymptotic stability is therefore guaranteed by (5.13) where

$$\gamma_I = \frac{1 - m_I^2}{b_I r_T h_I} > 0, \quad \gamma_A = \frac{1 - m_A^2}{b_A\,(r_A + r_T h_A)} > 0, \quad \gamma_T = \frac{1 - m_T^2}{b_T r_T\,(1 - h_A - h_I)} > 0. \tag{A.6}$$

The above inequalities hold in view of the information of Table 1 on the various mortalities and from (2.6) for γ_T. Further, note that $\zeta_{X-} < 0$ for all the populations $X \in \{I, A, T\}$ and, therefore, this lower bound is indeed excluded from the conditions (5.13).